Summary

Plate-scale deformation is expected to impart seismic anisotropic fabrics on the lithosphere. Determination of the fast shear wave orientation (ϕ) and the delay-time between the fast and slow split shear waves (δt) via SKS splitting can help place spatial and temporal constraints on lithospheric deformation. The Canadian Appalachians experienced multiple episodes of deformation during the Phanerozoic: accretionary collisions during the Paleozoic prior to the collision between Laurentia and Gondwana, and rifting related to the Mesozoic opening of the North Atlantic. However, the extent to which extensional events have overprinted older orogenic trends is uncertain. We address this issue through measurements of seismic anisotropy beneath the Canadian Appalachians, computing shear wave splitting parameters (ϕ, δt) for new and existing seismic stations in Nova Scotia and New Brunswick. Average δt values of 1.2 s, relatively short length-scale (≥100 km) splitting parameter variations, and a lack of correlation with absolute plate motion direction and mantle flow models, demonstrate that fossil lithospheric anisotropic fabrics dominate our results. Most fast directions parallel Appalachian orogenic trends observed at the surface, while δt values point towards coherent deformation of the crust and mantle lithosphere. Mesozoic rifting had minimal impact on our study area, except locally within the Bay of Fundy and in southern Nova Scotia, where fast directions are sub-parallel to the opening direction of Mesozoic rifting; associated δt values of >1 s require an anisotropic layer that spans both the crust

and mantle, meaning the formation of the Bay of Fundy was not merely a thin-skinned tectonic event.

Keywords:

102. Seismic anisotropy
111. Body waves
141. Continental tectonics: compressional
142. Continental tectonics: extensional
206. North America

Introduction

Plate scale deformation can lead to the development of an anisotropic fabric within the lithosphere (e.g. Helffrich, 1995) through the alignment of olivine crystals in the upper mantle (e.g., Bystricky et al., 2000; Tommasi et al., 2000; Zhang and Karato, 1995). When a shear wave travels through an anisotropic medium it is split into two orthogonal shear waves, one travelling faster than the other (e.g., Silver 1996). Measurements of the polarisation direction of the fast wave (ϕ) and the delay time between the fast and slow waves (δt) can then be used to characterise the anisotropic medium.

Core shear waves such as SKS and SKKS (hereafter referred to as SKS) are well suited for studying shear wave splitting and the anisotropic properties of the upper mantle directly beneath a seismic station. They are radially polarised, P-to-S conversions formed at the core-mantle boundary that preserve no source-side anisotropy (Long and Silver 2009, Savage 1999).

The Canadian Appalachians have experienced multiple episodes of deformation during the Phanerozoic (e.g. van Staal and Barr, 2012). A series of Paleozoic accretionary collisions took place on the margin of Laurentia, prior to the Laurentia-Gondwana collision that formed the supercontinent Pangea. In the Mesozoic, rifting related to the opening of the North Atlantic affected the eastern edge of this region, one consequence of which was the formation of the Bay of Fundy (e.g., Withjack et al., 1995) (Figure 1).

Previous studies of shear-wave splitting parameters in southeast Canada revealed little correspondence between orientations of anisotropic fabrics and asthenospheric flow beneath the Canadian Appalachians (Darbyshire et al., 2015). Fossil lithospheric anisotropic fabrics are thus likely to exert first order control on the observations. However, data from only a small number of seismic stations in the Canadian Appalachians have been used to establish this hypothesis, rendering the plate-scale tectonic evolution of the region poorly constrained in space and time. For example, whether or not the Mesozoic formation of the Fundy Basin was a thin-skinned, 'crustal' event, or one that also affected the mantle lithospheric mantle, remains poorly understood.

To address these issues, we analyse broadband seismic data from a combined network of new and existing seismic stations centred on the Bay of Fundy, to compute shear wave splitting parameters (ϕ, δt) for the region. After consideration of proposed mantle flow directions from absolute plate motion (APM) and geodynamic modelling results (Darbyshire et al., 2015), we compare the orientation of the fast direction to geological trends from the Appalachian orogenies, rifting in the Bay of Fundy, and extension related to the opening of the North Atlantic. In doing so, we assess the orientation and depth extent of deformation and whether rifting-related anisotropic fabrics have overprinted older orogenic anisotropic fabrics.

Tectonic setting

The Canadian Appalachians formed from the accretion of a series of oceanic arcs and continental fragments to the southeast margin of Laurentia during the Paleozoic. The region can be divided into five principal tectonostratigraphic zones (Williams, 1979) (Figure 1), although it should be noted that some comprise distinct tectonic elements themselves (e.g., van Staal and Barr, 2012). To the northwest the Humber Margin, was the edge of Laurentia when Dunnage zone material was accreted during the Ordovician, closing the Taconic Seaway.

Both zones comprise material that was on the Laurentian side of the Iapetus Ocean.

The three southeastern zones, Ganderia, Avalonia and Meguma, were continental fragments that separated from Gondwana during the Early Paleozoic. Ganderia collided with the composite edge of Laurentia during the Silurian, closing the Iapetus Ocean, and Avalonia accreted during the Early Devonian Arcadian Orogeny. Finally, Meguma, a terrane only found in present-day southern Nova Scotia, collided with the Avalonian edge of Laurentia in the Carboniferous.

Terminal collision between Laurentia and Gondwana occurred in the Mid-Carboniferous and Early Permian during the Alleghanian Orogeny, and led to the formation of the supercontinent Pangea. The Canadian Appalachians were relatively unaffected by Alleghanian Orogeny deformation (van Staal and Barr, 2012) and are thus a good location to study structures related to the earlier accretionary tectonic phases.

During the Mid-Triassic to Early Jurassic, NW-SE oriented rifting formed the Bay of Fundy (Withjack et al. 1995, Withjack et al. 2010). Rifting reactivated Paleozoic thrusts as normal faults, and resulted in the deposition of synrift non-marine sedimentary rocks and the eruption of tholeiitic basalts (Withjack et al. 1995). Fundy Basin extension ceased with the opening of the North Atlantic in the Early-to-Mid Jurassic. The rifted margin shows variation off-shore of Nova Scotia: the margin is volcanic to the southwest, but non-volcanic to the northeast of Nova Scotia and Newfoundland (Keen and Potter et al., 1995; Funck et al.,

2004). Since the Cretaceous, the Canadian Appalachians have been tectonically quiet.

Data and Methods

We use data from nineteen broadband seismic stations deployed in the Canadian Appalachians (Table 1, Figure 1) in Nova Scotia, New Brunswick, Newfoundland and Quebec. Of these, nine stations are from the Imperial College Maritimes network in Nova Scotia and New Brunswick, deployed between September 2013 and August 2015. These stations consisted of Güralp CMG-3TP seismometers with associated Güralp digitisers and GPS timing. The remaining stations consist of six temporary POLARIS stations (Portable Observatories for Lithospheric Analysis and Research Investigating Seismicity: Eaton et al., 2005) that operated for periods of 2-3.5 years, and four permanent stations from the Canadian National Seismograph Network (CNSN).

Earthquakes that occurred between October 2005 and October 2015, with magnitudes ≥6.0 and epicentral distances ≥88° were selected from the global catalogue. This distance range was chosen to isolate SKS core phases from other direct S phases to focus our analysis on receiver-side mantle anisotropy. Seismograms were filtered using a zero-phase, two-pole, Butterworth band-pass filter with corner frequencies 0.04 and 0.3 Hz. Seismograms were visually

inspected and waveforms with high signal-to-noise ratio, where an SKS or SKKS phase was clearly visible, were selected for further analysis.

When an SKS phase exhibits shear wave splitting, particle motion is elliptical because a proportion of the energy exists on the tangential component (e.g. Figure 2). If shear wave splitting does not occur, the particle motion will be linear and no energy appears on the tangential component, resulting in a 'null' measurement (e.g. Figure 3). A null may result from the material that the wave passes through being azimuthally-isotropic, multiple layers of anisotropy cancelling out (Barruol and Hoffmann, 1999), or if the backazimuth of the incoming earthquake is parallel or perpendicular to the fast polarisation direction.

We measure the fast polarisation direction (ϕ) and the delay time between the fast and slow shear waves (δt) using the approach of Teanby et al., (2004), which is based on the methodology of Silver and Chan (1991). Horizontal-component seismograms are rotated and time-shifted to minimise the second eigenvalue of the covariance matrix for particle motion within a window around the SKS phase. This is equivalent to linearising particle motion, and minimising the energy on the tangential component seismogram. We make measurements for 100 different windows around the SKS phase, and use cluster analysis to determine the most stable splitting parameters. Only measurements where the difference between the back-azimuth and source polarisation direction of the SKS phase is $\leq 20°$ are accepted, thus avoiding spurious results that could be

associated with anomalies in the deep lower mantle (e.g., Restivo and Helffrich, 2006). We obtain 40 high quality split measurements and 30 null measurements from 25 earthquakes (Tables S1 and S2, Figure 4). It should be noted that many of the seismic stations were located close to the coast, in a relatively high noise environment, and some stations (e.g. ALLY, JOSY, MANY) only operated for the short timespan of ~1 year.

Results

Figure 2 shows an example of a split measurement from station EDEY; Figure 3 is an example null measurement from station SJNN. Splitting parameters for individual station-event pairs are shown in Figures S1-4 and summarised in Figure S5 and Table S2.

At stations where splitting parameters show no significant backazimuthal variation, mantle anisotropy is characterised as a single, homogenous, horizontal layer; we thus adopt the stacking approach of Restivo and Helffrich (2006) to obtain a single pair of splitting parameters. Data coverage is insufficient to resolve the complex patterns of shear wave splitting variation associated with multiple or dipping anisotropic layers.

Results are summarised in Figure 4 and Table 1. Delay times range from 0.7 s (TIGG) to 1.85 s (MALG), but most fall within δt=0.9-1.4 s. Consistent fast

directions can be observed within some groups of stations on a 200-300 km length-scale, but changes over short distances (<100 km) are also evident. One of the most striking is the change from a SE-NW fast direction for stations ALLY (southern Nova Scotia) and MANY (Bay of Fundy) to a SW-NE fast direction for stations in southern New Brunswick (Figure 4). Fast directions across northern Nova Scotia are generally ~WSW-ENE, but those observed for stations CHEG (Cape Breton Island) and TIGG (Prince Edward Island) are NW-SE. The fast direction changes once again to SW-NE on the southern tip of Newfoundland (Figure 4).

At stations SABG, JOSY, MADG, SJNN and DRLN only null measurements were found. For JOSY, MADG and DRLN, the earthquake backazimuths yielding these results were either parallel or perpendicular to the fast directions observed at neighbouring stations (ALLY and MANY, TIGG and CHEG, and CODG respectively). Given the 90° ambiguity inherent in null measurements, it is reasonable to assume that the null directions are either perpendicular or parallel to the fast direction of anisotropy at these stations. However, the limited backazimuthal coverage means we cannot preclude the presence of multiple, cancelling layers of anisotropy (e.g., Barruol & Hoffmann, 1999) beneath these stations.

Discussion

Causes of seismic anisotropy and comparisons with previous studies

Seismic anisotropy in the Earth results from the alignment of minerals in the crust and/or mantle, the preferential alignment of fluid or melt (e.g., Blackman and Kendall, 1997), alternating sequences of sub-parallel layers of rocks of different seismic velocities (periodic transverse layering; Backus, 1962), or some combination thereof. We exclude melt alignment as a source of anisotropy in the Canadian Appalachians, since the region last experienced magmatism during the Mesozoic (van Staal and Barr, 2012). Mantle anisotropy therefore most likely results from the alignment of olivine crystals, olivine being the most abundant mineral in the upper mantle and highly anisotropic. Shear stresses can lead to the development of crystallographic preferred orientation (CPO) of olivine, where the a-axis is aligned to an orientation related to deformation (e.g., Bystricky et al., 2000; Tommasi et al., 2000; Zhang and Karato, 1995).

Processes that could lead to the development of anisotropic fabric include: asthenospheric flow in the direction of APM (e.g., Bokelmann and Silver, 2002), asthenospheric flow around a cratonic root (e.g., Assumpção et al., 2006; Bormann et al., 1993), and frozen-in fossil anisotropy within the lithosphere from the last deformation event (e.g., Bastow et al., 2007; Silver and Chan, 1988; Vauchez and Nicolas, 1991).

Periodic transverse layering is likely a source of anisotropy at crustal depths, however the continental crust typically only accounts for only 0.1-0.3 s (Silver, 1996) or 0.1-0.5 s (Barruol and Mainprice, 1993) of SKS splitting observations, so our δt values (mean δt=1.2 s) require a mantle contribution. Estimates of anisotropic layer thickness can be made from the relationship $L \approx (\delta t * Vs)/dVs$ (e.g., Helffrich, 1995), where L is layer thickness, Vs is shear velocity, and dVs is average percentage anisotropy. Taking a dVs of 4%, an upper limit of the degree of anisotropy prevalent in the upper 200 km of the Earth, (Savage, 1999) and a Vs in the range 4.48 km/s (mantle velocities from ak135, Kennett et al. 1995) to 4.65 km/s (average cratonic lithospheric mantle velocities in SE Canada (Schaeffer and Lebedev, 2014, Yuan et al., 2014)), our mean δt=1.2 s corresponds to a layer thickness of 134-140 km, not dissimilar to the ~150-175 km estimates for lithospheric thickness in the Canadian Appalachians (Schaeffer and Lebedev, 2014). Similarly, if we assume that the average 1.2 s of splitting we observe is accrued in the region's 150-175 km thick lithosphere (e.g., Schaeffer and Lebedev, 2014), the uppermost mantle beneath our network would be, on average, 3.1-3.7% anisotropic, a reasonable estimate for lithospheric anisotropy when compared to other studies worldwide (e.g. Savage, 1999). Further, the distances over which splitting parameters change (in several cases <100 km) is smaller than the width of the first Fresnel zone at the base of the lithosphere (~150 km).

There are four published SKS splitting measurements in our study area from Darbyshire et al. (2015) (Figure 4, Table 1). These show good agreement with the results we obtain from nearby stations. The nearest station to our region

analysed by Barruol et al. (1997) (station CBM in Maine) has a similar fast direction to that of station HOLY, and is sub-parallel to the strike of Paleozoic Appalachian orogenic structures.

Many of the ϕ measurements obtained from the northern US Appalachians to the southwest of our study region by Barruol et al. (1997) are E-W oriented. Subsequent modelling of anisotropy in the New England region (Levin et al., 1999; Levin et al., 2000; Yuan and Levin, 2014) finds that it is best explained by two distinct layers: a lower layer in the asthenosphere paralleling APM, and an upper layer in the lithosphere that is perpendicular to the main geological trends in the region. It is argued that this upper layer may be a result of a fabric developed due to the loss of the lower part of the lithosphere at some point after the assemblage of the Appalachians. Multiple layers of anisotropy, including the presence of anisotropy in the lithosphere, are further supported by estimates of anisotropic parameters made using splitting measurements and full waveform analysis (e.g., Yuan and Romanowicz, 2010; Yuan et al., 2011).

Long et al. (2015) recently conducted an SKS splitting study of the eastern US using data from the Transportable Array seismic stations. In the southern Appalachians, from Alabama to Pennsylvania, they see a strong correlation between ϕ and the strike of the mountain chain, including a rotation in ϕ coincident with a bend in topography. They argue in this region that the primary contribution to anisotropy is from the lithosphere. In the region closest to our study region, directly to the west and south, their results are more complex. Averaged over a relatively large area, the average ϕ direction is 77°, however

there is significant variation over relatively short distances, which they also argue suggests a lithospheric component to the observed anisotropy. In neither of these two regions do they observe a consistent alignment to APM.

Role of plate motion and mantle flow

Splitting measurements from southern New Brunswick and southern Newfoundland show some agreement with the APM direction from the HS3-NUVEL 1A (hotspot) model (Gripp and Gordon, 2002), however there is no consistent correlation with APM direction across the whole region. Similarly, while the fast direction observed in southern Nova Scotia and in the Bay of Fundy parallels the NNR-MORVEL (no-net-rotation) model (DeMets et al., 2010) there is again no consistent correlation throughout the Maritimes. Furthermore, the North American Plate is moving relatively slowly (17-22 mm/yr), slower than the ~40 mm/yr that Debayle and Ricard (2013) suggest is the necessary plate velocity for basal drag fabrics to develop based on their global comparison of APM and anisotropic fast directions. Anisotropy resulting from APM is, therefore, unlikely to be the dominant cause of the observed anisotropy.

Darbyshire et al. (2015) compare splitting parameters to mantle flow predictions of Forte et al. (2015). In the model that best simulates the lithospheric thickness in Appalachian Canada, radial flow dominates over horizontal flow. This would result in null measurements for the majority of seismic stations in this region: this clearly is not the case for most stations. Taking into account our estimates of anisotropic layer thickness and the lack of correlation of APM directions and

mantle flow models, a fossil lithospheric hypothesis for Canadian Appalachian mantle anisotropy seems most appropriate.

Backazimuthal coverage of our splitting measurements is limited to a relatively narrow range (Figures S1-S4). Studies with better backazimuthal representation are usually associated with stations that operated for much longer than the 1-3 years to which we have access (e.g., Levin et al., 2000). Although our interpretations are necessarily limited to a single homogenous, horizontal layer of anisotropy, we cannot preclude the possibility of dipping or multiple layers of anisotropy, including an asthenospheric component (e.g. Levin et al., 2000; Silver and Savage, 1994).

Relationship with tectonic structures

Fast polarisation directions in the Canadian Appalachians are mostly parallel or subparallel to geological trends from the Paleozoic Appalachian orogenies (Figure 1). Variations, such as between those in southern New Brunswick and those in Nova Scotia, and between Prince Edward Island, New Brunswick and Newfoundland follow variations in the strike of the boundaries between the different tectonic zones. Agreement between Appalachian trends and fast directions has also been documented elsewhere in the orogen by Long et al. (2015) and in earlier work by Barruol et al. (1997). Further, previous SKS splitting studies from other old orogenic belts, such as the Caledonian trends in the UK and Ireland (e.g. Helffrich 1995; Bastow et al., 2007) have also noted that

olivine CPO tends to parallel the strike of these belts. Much of the anisotropy we observe is thus related to Appalachian tectonic deformation. Splitting delay times of $\delta t > 1$ s point towards plate-scale deformation, coherent in the crust and lithospheric mantle.

The NW-SE fast direction at station MANY in the Bay of Fundy is at a high angle to the trend of Appalachian structures. The Bay of Fundy underwent rifting in a NW-SE direction during the Mid-Triassic to Early Jurassic (e.g. Withjack et al. 1995); extensional deformation may thus have over-printed older Appalachian trends. In magma-rich rifts, fast directions are typically rift-parallel (e.g., Kendall et al., 2006), but in magma-poor rifts such as the Rhine Graben (Vinnik et al., 1992) and the Baikal rift (Gao et al., 1997), they tend to be rift-perpendicular. This is due to the lattice-preferred orientation of lithospheric mantle olivine crystals induced by plate stretching (Nicolas and Christensen, 1987). Withjack et al. (1995) suggest the Fundy Basin experienced compression in a NW-SE direction from the Early Jurassic to Early Cretaceous. Unlike the earlier rifting, this does not seem to have influenced the lithospheric mantle.

The fast direction for MANY is slightly oblique (~25°) to the Bay of Fundy paleo opening direction. Obliquity between the strike of normal fault networks and opening directions is not uncommon during the development of continental breakup, however. For example, Corti et al., (2008) observe a ~20° obliquity in the tectonically active Ethiopian rift. Our observations are thus consistent with the hypothesis that, in the Bay of Fundy, Mesozoic plate-scale extensional tectonics over-printed older Appalachian fossil lithospheric anisotropic fabrics.

The fast direction at ALLY on the Atlantic coast of southern Nova Scotia is similar to MANY, but ~30° different to HAL, also located on Nova Scotia's Atlantic coast. The observations at ALLY may, like MANY, be the result of Mesozoic rifting. Although we cannot constrain them, along-axis variations in the strength of the continental lithosphere may explain our observations: weaker lithosphere to the south where the Bay of Fundy formed; stronger lithosphere to the north. Offshore rifted margin structure lends some support to this hypothesis: seaward dipping reflector sequences are prevalent along the margin in the south, but missing further northeast (Keen and Potter et al., 1995). Funck et al. (2004) argue that the Nova Scotian margin becomes increasingly non-volcanic to the northeast, also implying a change in extensional processes along-strike. Regardless of the governing factor, we conclude that Mesozoic extensional deformation of the lithosphere in the Canadian Maritimes was plate-scale but localised in nature.

Conclusions

SKS splitting measurements are made at nineteen broadband seismic stations in the Canadian Appalachians. Improved station numbers and density compared to previous studies in this region means we are better able to constrain spatial and

temporal variations in lithospheric deformation. The length scale of variations (~100 km), average δt of 1.2 s, and the lack of correlation with APM directions and asthenospheric flow models suggests that frozen-in lithospheric fabrics dominate the anisotropy in the region. There is good agreement between the fast polarisation directions at most stations and surface geological trends related to the Appalachian orogenies. Paleozoic accretionary collisions thus likely deformed the crust and the mantle lithosphere coherently. Later Mesozoic rifting had minimal impact on the Canadian Appalachians outside of the Bay of Fundy and southern Nova Scotia. In these areas, fast directions do not follow Appalachian trends, but are sub-parallel to the direction of rifting in the Mesozoic. This suggests that Mesozoic rifting affected the entire lithosphere beneath the Bay of Fundy, not just the crust, but its influence was confined to this relatively small area.

Acknowledgements

This work was funded by Leverhulme Trust research project grant RPG-2013-332. Imperial College Maritimes network stations were provided through NERC Geophysical Equipment Facility loan 986. Logistical field support was provided by D. Heffler, D. Simpson and residents of Nova Scotia and New Brunswick. Data for POLARIS and CNSN stations were downloaded from the Canadian National Data Centre. POLARIS stations were funded by the Canadian Foundation for Innovation, Natural Resources Canada and Industry Canada. F.D. is supported by

NSERC through the Discovery Grants and Canada Research Chair programmes. A.B. is funded by the NERC Doctoral Training Partnership: Science and Solutions for a Changing Planet. We thank Thomas Plenefisch and an anonymous reviewer for their comments on this manuscript.

References

Assumpção, M., Heintz, M., Vauchez, A., & Silva, M. E. (2006). Upper mantle anisotropy in SE and Central Brazil from SKS splitting: evidence of asthenospheric flow around a cratonic keel. *Earth and Planetary Science Letters*, *250*(1), 224-240. doi:10.1016/j.epsl.2006.07.038

Backus, G. E. (1962), Long-wave elastic anisotropy produced by horizontal

layering, *Journal of Geophysical Research*, 67, 4427– 4440.

Barruol, G., & Mainprice, D. (1993). A quantitative evaluation of the contribution of crustal rocks to the shear-wave splitting of teleseismic SKS waves. *Physics of the Earth and Planetary Interiors*, *78*(3), 281-300. doi:10.1016/0031-9201(93)90161-2

Barruol, G., Silver, P. G., & Vauchez, A. (1997). Seismic anisotropy in the eastern United States: deep structure of a complex continental plate. *Journal of Geophysical Research, 102*, 8329-8348. doi: 10.1029/96JB03800

Barruol, G., & Hoffmann, R. (1999). Upper mantle anisotropy beneath the Geoscope stations. *Journal of Geophysical Research*, *104*(B5), 10757-10. doi: 10.1029/1999JB900033

Bastow, I. D., Owens, T. J., Helffrich, G., & Knapp, J. H. (2007). Spatial and temporal constraints on sources of seismic anisotropy: Evidence from the Scottish highlands. *Geophysical Research Letters*, *34*, L05305, doi:10.1029/2006GL028911

Blackman, D. K., & Kendall, J. M. (1997). Sensitivity of teleseismic body waves to mineral texture and melt in the mantle beneath a mid–ocean ridge. *Philosophical Transactions of the Royal Society of London A: Mathematical, Physical and Engineering Sciences*, *355*(1723), 217-231. doi: 10.1098/rsta.1997.0007

Bokelmann, G., and Silver, P., 2002, Shear stress at the base of shield lithosphere: *Geophysical Research Letters, 29(23)*, 2091, doi: 10.1029/2002GL015925.

Bormann, P., Burghardt, P. T., Makeyeva, L. I., & Vinnik, L. P. (1993). Teleseismic shear-wave splitting and deformations in Central Europe. *Physics of the Earth and Planetary Interiors*, *78*(3), 157-166. doi:10.1016/0031-9201(93)90153-Z

Bystricky, M., Kunze, K., Burlini, L., & Burg, J. P. (2000). High shear strain of olivine aggregates: rheological and seismic consequences. *Science*, *290*(5496), 1564-1567. doi: 10.1126/science.290.5496.1564

Corti, G. (2008). Control of rift obliquity on the evolution and segmentation of the main Ethiopian rift. *Nature Geoscience*, *1*(4), 258-262. doi:10.1038/ngeo160

Darbyshire, F. A., Bastow, I. D., Forte, A. M., Hobbs, T. E., Calvel, A., Gonzalez-Monteza, A., & Schow, B. (2015). Variability and origin of seismic anisotropy across eastern Canada: evidence from shear-wave splitting measurements. *Journal of Geophysical Research*, *120*, doi:10.1002/2015JB012228

Debayle, E., & Ricard, Y. (2013). Seismic observations of large-scale deformation at the bottom of fast-moving plates. *Earth and Planetary Science Letters*, *376*, 165-177. doi:10.1016/j.epsl.2013.06.025

DeMets, C., Gordon, R. G., & Argus, D. F. (2010). Geologically current plate motions. *Geophysical Journal International*, *181*(1), 1-80. doi: 10.1111/j.1365-246X.2009.04491.x

Eaton, D. W., Adams, J., Asudeh, I., Atkinson, G. M., Bostock, M. G., Cassidy, J. F., Ferguson, I., Samson, C., Snyder, D., Tiampo, K.F.., & Unsworth, M. J. (2005). Investigating Canada's lithosphere and earthquake hazards with portable arrays. *Eos, Transactions American Geophysical Union*, *86*(17), 169-173. doi: 10.1029/2005EO170001

Forte, A. M., Simmons, N. A., & Grand, S. P. (2015). Constraints on seismic models from other disciplines—Constraints on 3-D seismic models from global geodynamic observables: Implications for the global mantle convective flow. *Treatise of Geophysics*, *1*, 853-907.

Funck, T., Jackson, H. R., Louden, K. E., Dehler, S. A., & Wu, Y. (2004). Crustal structure of the northern Nova Scotia rifted continental margin (eastern Canada). *Journal of Geophysical Research*, *109*, B09102, doi:10.1029/2004JB003008

Gao, S., Davis, P.M., Liu, H., Slack, P.D., Rigor, A.W., Zorin, Y.A., Mordvinova, V.V., Kozhevnikov, V.M. & Logatchev, N.A. (1997). SKS splitting beneath continental rift zones. *Journal of Geophysical Research ,102*(B10), 22781-22797. doi: 10.1029/97JB01858

Gripp, A. E., & Gordon, R. G. (2002). Young tracks of hotspots and current plate velocities. *Geophysical Journal International*, *150*(2), 321-361. doi: 10.1046/j.1365-246X.2002.01627.x

Helffrich, G. (1995). Lithospheric deformation inferred from teleseismic shear wave splitting observations in the United Kingdom. *Journal of Geophysical Research*, *100*(B9), 18195-18204. doi: 10.1029/95JB01572

Keen, C. E., & Potter, D. P. (1995). The transition from a volcanic to a nonvolcanic rifted margin off eastern Canada. *Tectonics*, *14*(2), 359-371. doi: 10.1029/94TC03090

Kendall, J. M., Pilidou, S., Keir, D., Bastow, I. D., Stuart, G. W., & Ayele, A. (2006). Mantle upwellings, melt migration and the rifting of Africa: insights from seismic anisotropy. *Geological Society, London, Special Publications*, *259*(1), 55-72. doi: 10.1144/GSL.SP.2006.259.01.06

Kennett, B. L. N., Engdahl, E. R., and Buland, R., (1995), Constraints on seismic velocities in the Earth from traveltimes. *Geophysical Journal International*, *122* (1): 108-124. doi: 10.1111/j.1365-246X.1995.tb03540.x

Levin, V., Menke, W., & Park, J. (1999). Shear wave splitting in the Appalachians and the Urals: a case for multilayered anisotropy. *Journal of Geophysical Research*, *104*(B8), 17975-17993. doi: 10.1029/1999JB900168

Levin, V., Park, J., Brandon, M. T., & Menke, W. (2000). Thinning of the upper mantle during late Paleozoic Appalachian orogenesis. *Geology*, *28*(3), 239-242. doi: 10.1130/0091-7613(2000) 28<239:TOTUMD> 2.0.CO;2

Long, M. D., Jackson, K. G., & McNamara, J. F. (2015). SKS splitting beneath Transportable Array stations in eastern North America and the signature of past lithospheric deformation. *Geochemistry, Geophysics, Geosystems*, 16, doi:10.1002/2015GC006088.

Long, M. D., & Silver, P. G. (2009). Shear wave splitting and mantle anisotropy: measurements, interpretations, and new directions. *Surveys in Geophysics*, *30*(4-5), 407-461. doi: 10.1007/s10712-009-9075-1

Nicolas, A. and Christensen, N. I. (1987) Formation of Anisotropy in Upper Mantle Peridotites - A Review, in *Composition, Structure and Dynamics of the Lithosphere-Asthenosphere System (eds K. Fuchs and C. Froidevaux),* 111-123, doi: 10.1029/GD016p0111

Restivo, A., & Helffrich, G. (2006). Core—mantle boundary structure investigated using SKS and SKKS polarization anomalies. *Geophysical Journal International*, *165*(1), 288-302. doi: 10.1111/j.1365-246X.2006.02901.x

Schaeffer, A. J., & Lebedev, S. (2014). Imaging the North American continent using waveform inversion of global and USArray data. *Earth and Planetary Science Letters*, *402*, 26-41. doi:10.1016/j.epsl.2014.05.014

Savage, M. K. (1999). Seismic anisotropy and mantle deformation: what have we learned from shear waves. *Reviews of Geophysics*, *37*(1), 65-106. doi: 10.1029/98RG02075

Silver, P. G., & Chan, W. W. (1988). Implications for continental structure and evolution from seismic anisotropy. *Nature*, *335*, 34-39 doi:10.1038/335034a0

Silver, P. G., & Chan, W. W. (1991). Shear wave splitting and subcontinental mantle deformation. *Journal of Geophysical Research*, *96*(16), 16429-16454. doi: 10.1029/91JB00899

Silver, P. G., & Savage, M. K. (1994). The interpretation of shear-wave splitting parameters in the presence of two anisotropic layers. *Geophysical Journal International*, *119*(3), 949-963. doi: 10.1111/j.1365-246X.1994.tb04027.x

Silver, P. G. (1996). Seismic anisotropy beneath the continents: probing the depths of geology. *Annual Review of Earth and Planetary Sciences*, *24*, 385-432. doi: 10.1146/annurev.earth.24.1.385

Teanby, N. A., Kendall, J. M., & Van der Baan, M. (2004). Automation of shear-wave splitting measurements using cluster analysis. *Bulletin of the Seismological Society of America*, *94*(2), 453-463. doi: 10.1785/0120030123

Tommasi, A., Mainprice, D., Canova, G., & Chastel, Y. (2000). Viscoplastic self-consistent and equilibrium-based modeling of olivine lattice preferred orientations: Implications for the upper mantle seismic anisotropy. *Journal of Geophysical Research*, *105*(B4), 7893-7908. doi: 10.1029/1999JB900411

van Staal, C. R., & Barr, S. M. (2012). Lithospheric architecture and tectonic evolution of the Canadian Appalachians and associated Atlantic margin. *Tectonic styles in Canada: The LITHOPROBE perspective. Edited by JA Percival, FA Cook, and RM Clowes. Geological Association of Canada, Special Paper*, *49*, 41-95.

Vauchez, A., & Nicolas, A. (1991). Mountain building: strike-parallel motion and mantle anisotropy. *Tectonophysics*, *185*(3), 183-201. doi:10.1016/0040-1951(91)90443-V

Vinnik, L. P., Makeyeva, L. I., Milev, A., & Usenko, A. Y. (1992). Global patterns of azimuthal anisotropy and deformations in the continental mantle. *Geophysical Journal International*, *111*(3), 433-447. doi: 10.1111/j.1365-246X.1992.tb02102.x

Williams, H. (1979). Appalachian orogen in Canada. *Canadian Journal of Earth Sciences*, *16*(3), 792-807. doi: 10.1139/e79-070

Withjack, M. O., Olsen, P. E. and Schlische, R. W. (1995). Tectonic evolution of the Fundy rift basin, Canada: evidence of extension and shortening during passive margin development. *Tectonics*, *14*(2), 390-405. doi: 10.1029/94TC03087

Withjack, M. O., Baum, M. S., & Schlische, R. W. (2010). Influence of preexisting fault fabric on inversion-related deformation: A case study of the inverted Fundy rift basin, southeastern Canada. *Tectonics*, *29*, TC6004, doi:10.1029/2010TC002744

Yuan, H., & Romanowicz, B. (2010). Lithospheric layering in the North American craton. *Nature*, *466*(7310), 1063-1068. doi:10.1038/nature09332

Yuan, H., Romanowicz, B., Fischer, K. M., & Abt, D. (2011). 3-D shear wave radially and azimuthally anisotropic velocity model of the North American upper mantle. *Geophysical Journal International*, *184*(3), 1237-1260. doi: 10.1111/j.1365-246X.2010.04901.x

Yuan, H., & Levin, V. (2014). Stratified seismic anisotropy and the lithosphere-asthenosphere boundary beneath eastern North America. *Journal of Geophysical Research*, *119*(4), 3096-3114. doi: 10.1002/2013JB010785

Yuan, H., French, S., Cupillard, P. & Romanowicz, B., 2014. Lithospheric expression of geological units in central and eastern North America from full waveform tomography. *Earth and Planetary Science Letters*, 402, 176-186. doi:10.1016/j.epsl.2013.11.057

Zhang, S., & Karato, S. I. (1995). Lattice preferred orientation of olivine aggregates deformed in simple shear. *Nature*, *375*(6534), 774-777. doi:10.1038/375774a0

Tables

Table 1: Stacked split results

Station	Net	Lat (°)	Lon (°)	ϕ(°)	σ_ϕ (°)	δt (s)	σ_{dt}	#	Data period
ALLY	IC	43.74	-65.10	-84	1.25	1.43	0.05	2	09/2013-07/2014; 05/2015-08/2015
CHEG	CNSN	46.81	-60.67	-56	12.75	1.00	0.23	1	10/2005-10/2015
CODG	POLARIS	47.84	-59.25	58	4.75	1.02	0.24	1	10/2005-10/2008
EDEY	IC	45.44	-62.32	83	1.75	1.23	0.03	5	09/2013-08/2015
HAL	CNSN	44.64	-63.59	67	2.5	0.90	0.02	4	08/2008-10/2015
HANN	POLARIS	45.88	-66.77	71	2.5	0.93	0.03	2	01/2013-10/2015
HOLY	IC	46.53	-66.46	33	2.5	1.40	0.08	3	09/2013-08/2015
MALG	POLARIS	45.79	-63.33	71	1	1.85	0.13	2	10/2005-10/2008
MALY	IC	45.79	-63.36	83	5.25	1.05	0.06	3	09/2013-08/2015
MANY	IC	44.69	-66.76	-75	1.5	1.48	0.03	3	09/2013-11/2013; 05/2014-08/2015
SHEY	IC	45.13	-61.99	-89	1.75	1.00	0.03	3	09/2013-08/2015
SUSY	IC	45.72	-65.43	58	5.00	1.23	0.06	2	09/2013-08/2015
TIGG	POLARIS	47.00	-64.00	-55	6.75	0.68	0.09	4	09/2005-11/2007
WODY	IC	45.10	-64.66	85	0.75	1.33	0.02	6	09/2013-

									08/2015
Splitting parameters from Darbyshire et al. (2015)									
BATG	POLARIS	47.23	-66.06	-86	5.00	0.53	0.03	6	
GBN	CNSN	45.41	-61.51	-84	1.50	0.68	0.03	7	
GGN	CNSN	45.12	-66.84	67	1.00	1.03	0.03	9	
LMN	CNSN	45.85	-64.81	76	1.75	1.15	0.06	5	

IC: *Imperial College Maritimes network*

POLARIS: *Portable Observatories for Lithospheric Analysis and Research Investigating Seismicity*

CNSN: *Canadian National Seismograph Network*

#: *Number of splitting measurements used in a stack*

σ: *one standard deviation*

The splitting parameters obtained for individual events can be found in Table S1; null events are recorded in Table S2

Figures

Figure 1

Locations of broadband seismic stations (magenta triangles), boundaries separating the Humber, Dunnage, Gander, Avalon and Meguma regions (thin black lines) and the Appalachian Front (thick black line). Inset map shows the location of the study region, marked as a red box, within eastern North America. QC – Quebec, NB – New Brunswick, NS- Nova Scotia, PEI – Prince Edward Island, CBI – Cape Breton Island, NF – Newfoundland, BoF – Bay of Fundy.

Figure 2

An example of a good splitting measurement at station EDEY. (a) The original three component seismogram showing the SKS phase and the window used. (b) The radial and tangential components before (top two) and after correction (bottom two). There is no energy on the corrected tangential component. (c) Top three images show the match between the fast (dashed line) and slow (solid line) waveforms: left is prior to correction (amplitudes normalised) and centre and right are after correction, normalised and true amplitudes respectively. The bottom two images show the elliptical particle motion prior to correction (left) and the linearised particle motion after correction (right). (d) Error and uncertainty calculation (contour labels indicate multiples of one sigma). Here a stable result and a well constrained 95% confidence contour (thick line) indicate a robust measurement. (e) Measurements of ϕ and δt obtained from 100 different analysis windows plotted against window number. (f) Cluster analysis of splitting parameters obtained from the 100 windows. Good results are stable over a large number of windows. In (d), (e) and (f) the star marks the values of ϕ and δt taken for this station/event pair.

Figure 3

An example of a null result at the station SJNN. (a)-(f) as in Figure 2. Note in (b) the lack of energy on the tangential component before and after correction and in (c) the linear particle motion before and after analysis.

Figure 4

Stacked shear wave splitting parameters from the stations in this study (purple bars) and from Darbyshire et al. (2015) (cyan bars). Red bars are null measurements. APM: absolute plate motion from the HS3-Nuvel-1A model of Gripp and Gordon (2002) in the hotspot reference frame (black arrow) and the NNR-MORVEL (no-net-rotation) model of DeMets et al. (2010) (green arrow). Inset map shows the location of earthquakes used; red stars are events where null measurements were obtained and purple stars are events where split measurements were obtained.

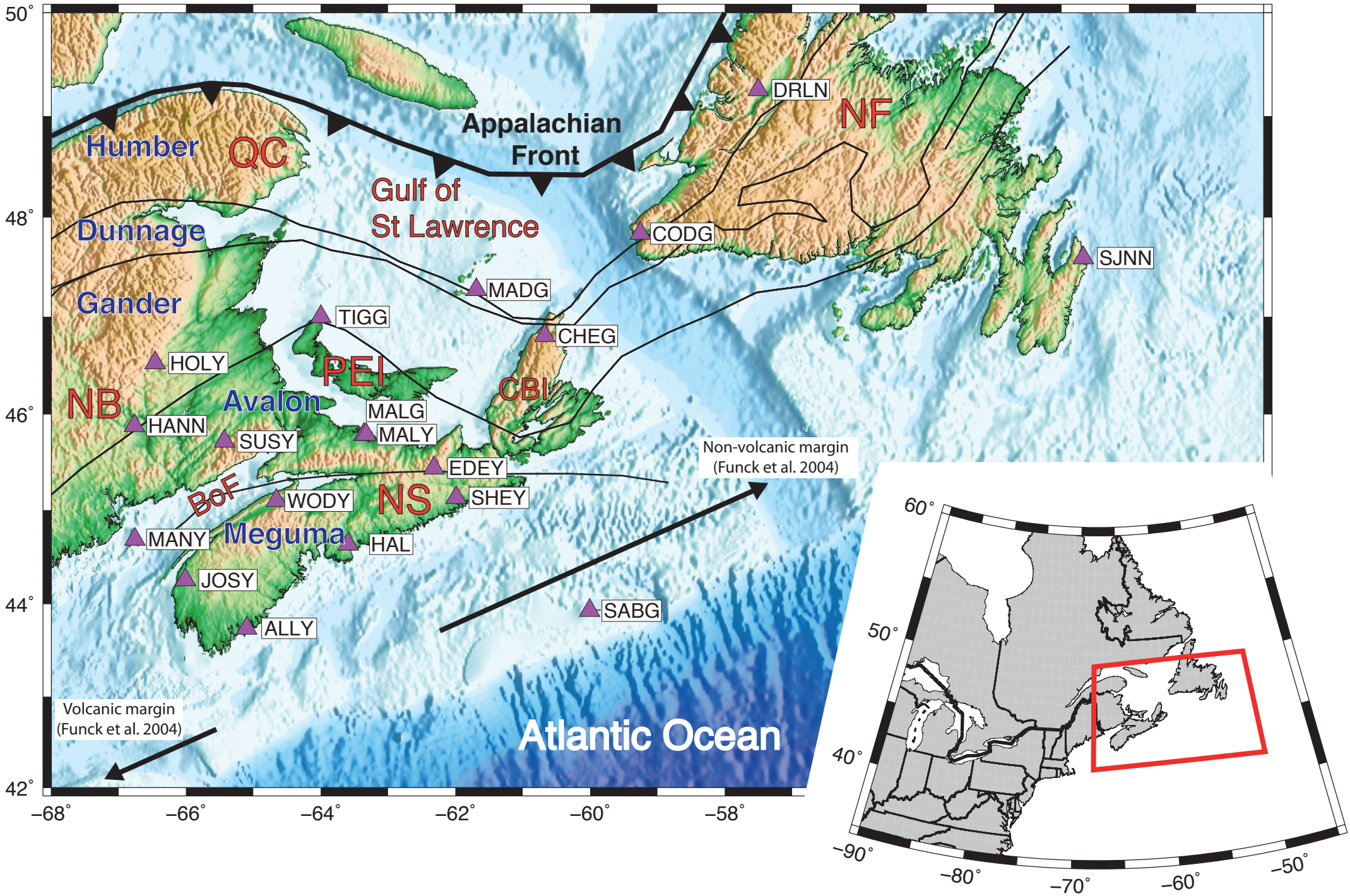
Appalachian Front
Humber
QC
Gulf of St Lawrence
Dunnage
Gander
NB
Avalon
PEI
CBI
NS
BoF
Meguma
NF
DRLN
CODG
SJNN
MADG
TIGG
CHEG
HOLY
HANN
SUSY
MALG
MALY
EDEY
WODY
SHEY
MANY
HAL
JOSY
ALLY
SABG
Non-volcanic margin (Funck et al. 2004)
Volcanic margin (Funck et al. 2004)
Atlantic Ocean
50°
48°
46°
44°
42°
−68°
−66°
−64°
−62°
−60°
−58°
60°
50°
40°
−90°
−80°
−70°
−60°
−50°

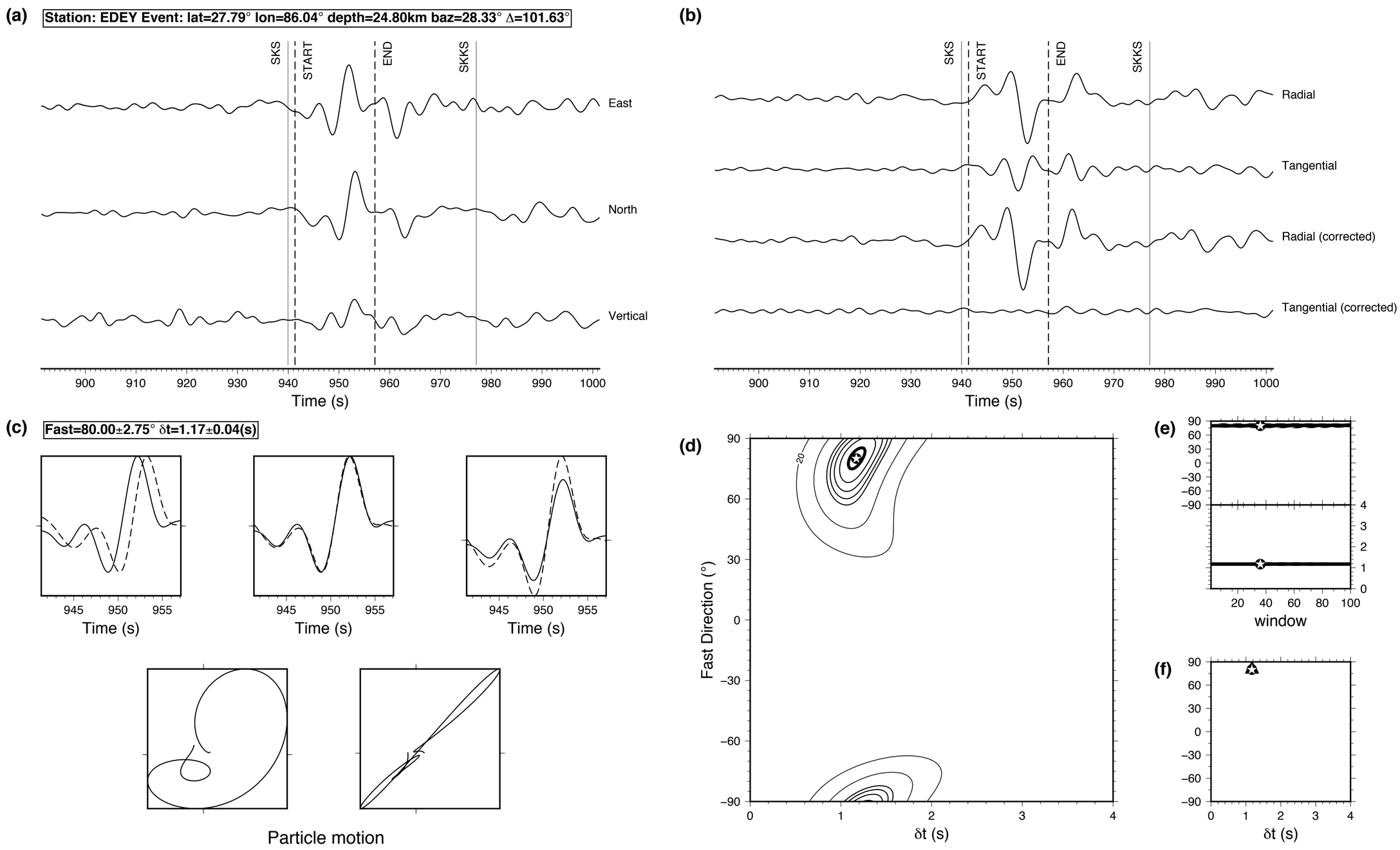
(a)
Station: EDEY Event: lat=27.79° lon=86.04° depth=24.80km baz=28.33° Δ=101.63°
SKS
START
END
SKKS
East
North
Vertical
900 910 920 930 940 950 960 970 980 990 1000
Time (s)
(b)
SKS
START
END
SKKS
Radial
Tangential
Radial (corrected)
Tangential (corrected)
900 910 920 930 940 950 960 970 980 990 1000
Time (s)
(c)
Fast=80.00±2.75° δt=1.17±0.04(s)
945 950 955
Time (s)
Particle motion
(d)
Fast Direction (°)
δt (s)
(e)
window
(f)
δt (s)

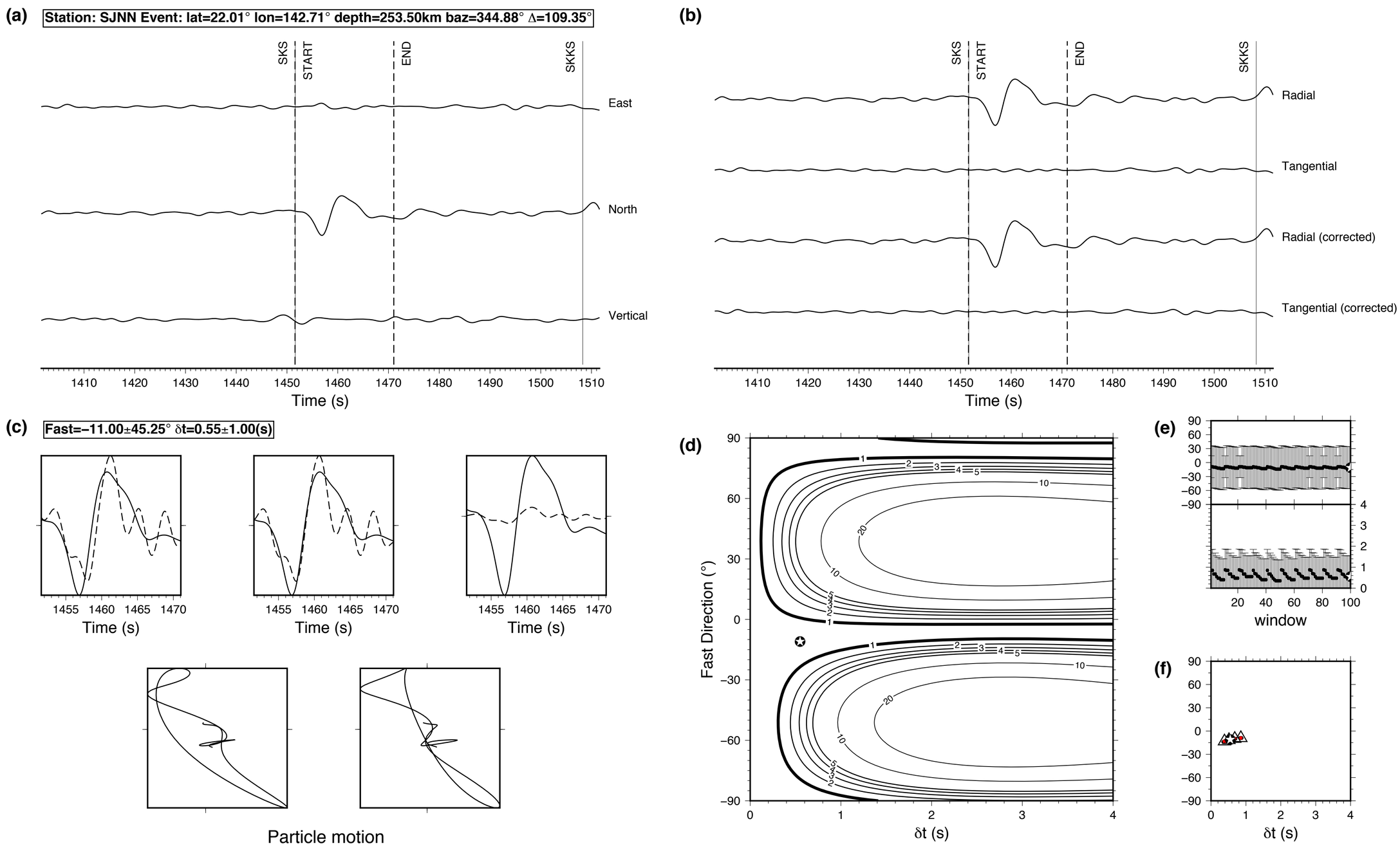
(a)
Station: SJNN Event: lat=22.01° lon=142.71° depth=253.50km baz=344.88° Δ=109.35°
SKS
START
END
SKKS
East
North
Vertical
1410 1420 1430 1440 1450 1460 1470 1480 1490 1500 1510
Time (s)
(b)
SKS
START
END
SKKS
Radial
Tangential
Radial (corrected)
Tangential (corrected)
1410 1420 1430 1440 1450 1460 1470 1480 1490 1500 1510
Time (s)
(c)
Fast=−11.00±45.25° δt=0.55±1.00(s)
1455 1460 1465 1470
Time (s)
Particle motion
(d)
Fast Direction (°)
δt (s)
(e)
window
(f)
δt (s)

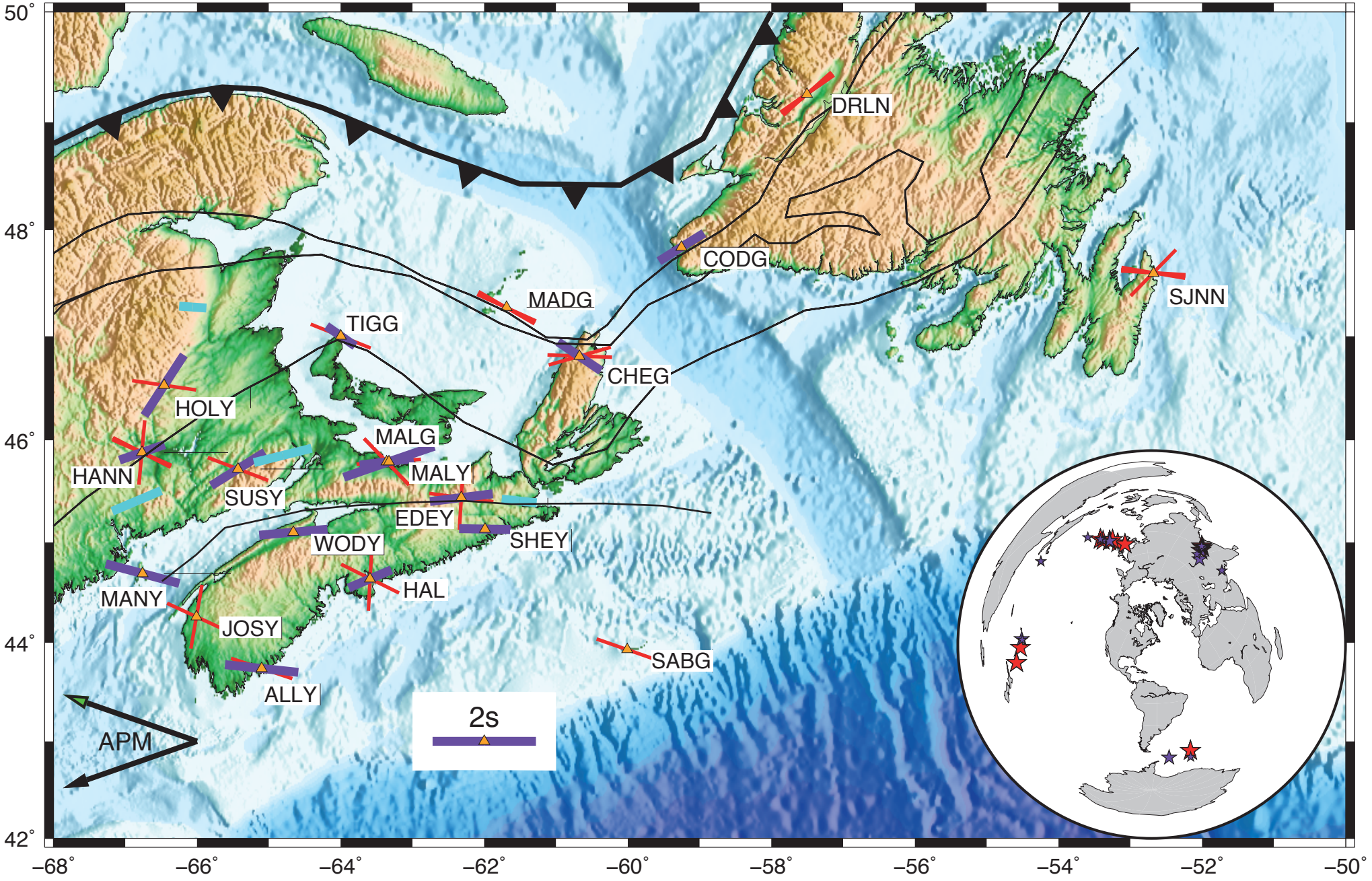
50˚
48˚
46˚
44˚
42˚
−68˚
−66˚
−64˚
−62˚
−60˚
−58˚
−56˚
−54˚
−52˚
−50˚
DRLN
CODG
SJNN
MADG
TIGG
CHEG
HOLY
MALG
HANN
MALY
SUSY
EDEY
SHEY
WODY
HAL
MANY
JOSY
SABG
ALLY
2s
APM